

Original Article

# Coyote Optimization Algorithm with Hybrid SVD-EVD Approach for Digital Image Watermarking

R. Parthiban<sup>1</sup>, S. Manikandan<sup>2</sup>

<sup>1</sup>Department of Computer Science, Government Arts and Science College, Kovilpatti, Thoothukudi.

<sup>2</sup>PG Department of Computer Science, Government Arts College, Chidambaram.

<sup>1</sup>Corresponding Author : parthiban.r68@gmail.com

Received: 05 March 2023

Revised: 11 April 2023

Accepted: 06 May 2023

Published: 31 May 2023

**Abstract** - The proliferation of digitalized media on the Internet has assisted in enhancing digitalization, which has increased copyright issues. To solve these copyright issues, digital watermarking methods were used. Digital image watermarking refers to a method in which watermark data is embedded into multimedia products and can be detected or extracted from the watermarked product later. Such techniques ensure content verification, tamper-resistance, integration, and image authentication. Therefore, this study develops a coyote optimization algorithm-based hybrid (COA-hybrid) model for digital Image watermarking. The presented COA-hybrid technique focuses on designing an effective image watermarking approach to fulfil the requirements of imperceptibility and robustness. In addition, the COA-hybrid model integrates the concepts of Singular Value Decomposition (SVD) and Eigen Value Decomposition (EVD). Here, the COA-hybrid technique embeds the watermarking on the DWT sub-band of the cover image. In addition, the watermarking's placed on the particular value components of the DWT sub-band of the cover imaging. Finally, the COA is utilized to adjust the parameters related to the hybrid model to increase fitness function. The simulation results of the COA-hybrid model are tested on different images, and the results reported the improvements of the COA-hybrid model over other models.

**Keywords** - Digital image watermarking, Image protection, Coyote optimization algorithm, Hybrid model, EVD, SVD.

## 1. Introduction

With the tremendous development of the World Wide Web (WWW) and the internet, it is very simple to transfer and disperse multimedia data like video, images, and audio through a single click [1]. It may also have some disadvantages since data is distributed and transmitted without the creator's knowledge, which results in many fraudulent cases. The unauthorized distribution and duplication demanded potential copyright protection tools [2]. In the past, the authors did it by hiding data patterns (data) or data within digital video, audio, and image files in different ways [3]. One way the data is hidden is in the digital signature format, digital watermark or copyright label that verifies the owner's identity and hence can be regarded as their intellectual property [4]. The method is called "Digital Watermarking", by which certain ownership data named watermark is concealed in the multimedia object so that the watermark is removed if it is essential for proving the object's rights. Watermarking can be "invisible" or "visible" [5].

Mainly, watermarking techniques are applied in two different domains [6]: transform domain that functions on different levels of image transformation, namely Stationary

Wavelet Transforms (SWTs) or Lifting Wavelet Transforms (LWTs) and Discrete Wavelet Transforms (DWTs), spatial domain focused on applying watermark embedding or extracting directly into host image dataset [7, 8]. Though such two fields presented special features leading to different qualities and outcomes, the current study displays robustness and better efficiency of transform domain-watermarking methods [9, 10]. The two main criteria to evaluate watermarking methods are imperceptibility, which mentions low visual variances of the watermarked Image and strength [11], which specifies the visual quality of the extracted watermarking technique under different situations. It is a trade-off between these two features; enhancing imperceptibility causes low and contrarily enhancing robustness [12]. Much current research has concentrated on optimization techniques to balance trade-offs by electing appropriate watermarking factors [13]. Particle swarm optimization (PSO), Heuristic evolutionary algorithms, and firefly algorithm had addressed among these optimization methods [14].

This study develops a coyote optimization algorithm-based hybrid (COA-hybrid) model for digital Image



watermarking. The presented COA-hybrid technique integrates the concepts of Singular Value Decomposition (SVD) and Eigen Value Decomposition (EVD). Here, the COA-hybrid technique embeds the watermarking on the DWT subband of the cover image. In addition, the watermarking's placed on the singular value components of the DWT subband of the cover imaging. Finally, the COA is utilized to adjust the parameters related to the hybrid model to increase fitness function. The simulation results of the COA-hybrid model are tested on different images.

## 2. Related Works

Sajeer and Mishra [15] present a secure, durable fusion-related hybrid MIW method. The technique primarily utilized Fast Filtering (FF) to combine two medical images from various modalities for forming the cover images. A first-level Redundant DWTs (RDWTs) were used on this host imaging to deploy the element with the greatest entropy. After a single level, DWT is used. Liu et al. [16] modelled a new image watermark technique depending on DWT, SVD and Heisenberg Decomposition (HD). First, the host imagery was disintegrated into various sub-bands with the aid of multiple-level DWT in the embedding procedure, and the resulting coefficients were utilized as the input for HD. In [17], an enhanced robust watermarking technique was introduced in DFT through spread spectrum, maximizing the main operation variables, predominantly coefficients of frequency and the amounts of bands, along with the watermarking strength feature leveraging PSO in combination with bit correction rate standards and visualization data fidelity.

Devi et al. [18] presented this work to offer security and authentication to aerial RS imageries sent online by the method through the SVD schemes and the redundant DWT (RDWT) for DIW. In particular, SC is implemented for the numerical optimisation of crucial variables. Likewise, SVD and 1-level RDWT were implemented on singular matrices and digital cover images of HL and LH sub-bands were selected for watermark embedding. In [19], the authors devise a safe and vigorous digitalized image watermarking method utilizing Redundant DWT (RDWT)-SVD hybrid transform. To make the presented method robust against attacks, 1-level RDWT is the chosen block, and the SVD decomposition is applied. Pallaw et al. [20] modelled a hybrid watermarking technique utilizing the randomized-SVD, Slantlet transforms, and optimization methods stimulated by the nature Firefly technique. The watermarking Image was encoded through the XOR encrypting approach. A wide-ranging examination reveals that the new method outpaces the prevailing SSIM, PSNR, and NC techniques. El-Kenawy et al. [21] devise a unique method for digital Image watermarking that uses dipper-throated optimization (DTO), discrete cosine transform (DCT), DWT, and stochastic fractal search (SFS) techniques. The presented method includes DWT computing on the cover images to mine its sub-elements.

## 3. The Proposed Model

In this article, we have presented a novel COA-hybrid model for the digital Image watermarking procedure. The presented COA-hybrid technique lies in developing an effective Image watermarking approach to fulfil the requirements of imperceptibility and robustness. Besides, the COA-hybrid model integrates the concepts of the SVD and EVD approaches. Fig. 1 depicts the overall process of the COA-hybrid method.

### 3.1. DTCWT Model

The critical characteristics of DTCWT are that its size component is translating invariants. DCT splits the coefficient of video blocks or frames into high, lower and mid-level frequencies [22]. Since the low-frequency part represents the foremost signalling energies of the frame, modifications towards it would considerably damage the video's perception qualities. Simultaneously, the high-frequency part mainly concentrates on the texture part and contour of the video, which might not be powerful from conventional attacks like noise and lossy compression. Thus, many DCT-based video watermark schemes adjust the intermediate frequency coefficient to accomplish the watermarking embedding. The CWT transforms has the disadvantage of poor perfect reconstruction, and The DWT transforms has poor direction selectivity and lack shift-invariance. DTCWT overcome the shortcomings of DWT and CWT through 2 filter trees such that slight variations in the input signal do not cause a significant change in the energy distribution of the DTCWT coefficient at different scales. In addition, DTCWT has good direction selectivity and perfect reconstruction and is shift invariance that is not existing in earlier DWT, DCT, DFT and other transformations. Therefore, the transforms are better suited for developing a video watermarking system that resists geometric attacks like scaling and rotation[23].

The D-DTCWT applied to a video frame might produce six sub bands respective to the six angle-related directional filtering outputs. The convolutional wavelet coefficient at different levels is shown as follows:

$$F_{l,d}(u_l, v_l) = |F_{l,d}(u_l, v_l)| e^{j\theta_{l,d}(u_l, v_l)} \quad (1)$$

In Eq. (1),  $d$  denotes the filter direction, viz., the six directional sub bands. Every single level comprises six higher sub-bands and a lower band in different directions.

### 3.2. Design of Hybrid SVD-EVD Model

SVD decomposition is one main focus of linear algebraic methods that could diagonalize arbitrary matrices. A DTCWT sub band refers to an array of favourable scalar terms considered a matrix [24]. Here the sub band is denoted as a matrix  $A$ , and the singular value decomposition on  $A$  is executed as represented in the following.

$$A = USV^H \quad (2)$$

Here the descendant diagonal elements of  $S$  have named the singular values of  $A$ ,  $U$  and  $V$  denoted orthogonal matrices, and  $S$  indicated a diagonal matrix.

In this study, the hybrid SVD-EVD model is derived by the integration of the EVD into the SVD approach. EVD is a mathematical procedure for decomposing a square matrix as its eigenvalues and eigenvectors. An eigenvector of matrix  $A$  is a non-zero vector  $x$  such that if the  $A$  is multiplied by  $x$ , the outcome is a scalar multiple of  $x$ . The scalar multiple is termed as the eigenvalue equivalent to the eigenvector. Specifically, when it takes a square matrix  $A$  and a non-zero vector  $x$ , afterwards, the vector  $x$  is an eigenvector of  $A$  if and only if there occurs a scalar  $\lambda$  such that  $Ax = \lambda x$ . EVD is utilized in many applications comprising quantum mechanics, signal processing, and data compression. It is suitable to diagonalise a matrix that means determining a basis of eigenvectors that generates the diagonal matrix. It simplifies calculations and exposes suitable properties of matrices. The EVD of a matrix  $A$  is written as:

$$A = Q\Lambda Q^{-1} \quad (3)$$

Whereas  $Q$  denotes the matrix whose columns are eigenvectors of  $A$ ,  $\Lambda$  represents the diagonal matrix whose entries are equal eigenvalues, and  $Q^{-1}$  refers to the inverse of  $Q$ . Noticeable, not every matrix is diagonalized utilizing EVD, and in some cases, difficult numbers can be contained in the eigenvector and eigenvalue.

### 3.3. Parameter Tuning using COA

The COA is utilized to adjust the parameters of the hybrid model. The COA is a population-based algorithm inspired by the behaviour of *Canis latrans* species called Coyote [25]. This algorithm does not rely on social grouping and dominates the rules over animals, contrasting with the Gray Wolf Optimizer (GWO). The leader of the hunting group can be signified as alpha. The population size of coyotes is divided into  $R_o \in R^*$  groups over  $R_b \in R^*$ . In each group, coyote was equal and balanced. Thus, the population size in the provided optimization technique can be obtained by the multiplication of  $R_o$  and  $R_b$ . The unstable coyote was dismissed for simplification at an early stage [26]. The critical contribution of the COA is the social structure and the robust algorithm for resolving optimization issues. The coyote behaviours form the basis of social location in implementing the coyote hunting system and can be stimulated by intrinsic and extrinsic elements.

$$sco_b^{o,s} = \vec{a} = (a_1, a_2, \dots, a_F) \quad (4)$$

The parameter  $\vec{a}$  Hunting can be denoted as the solution variance of global optimization problems. Therefore,  $sco$  can

be represented by social conditions,  $b^{th}$  as coyote,  $o^{th}$  are provided as a group in instant time  $s^{th}$ , and  $F$  denotes the search gap and also involves the coyote's adaption to the environment  $zks_b^{o,s} \in U$ . Fig. 2 illustrates the steps included in COA.

The initial hunting model of coyotes is used to prepare the entire population. The social constraint is randomly given to every coyote. The arbitrary value was assigned in the search space for  $b^{th}$  as coyote and  $o^{th}$  as pack of  $n^{th}$  dimension is shown in Eq. (5).

$$sco_b^{o,s} = vy_n + u_n \cdot (wy_n - vy_n) \quad (5)$$

The variables  $wy_n$  and  $uy_n$  are denoted as the lower and upper boundaries of  $n^{th}$  decision variance.  $u_n$  Indicates that the arbitral value ranges from zero to one. The adaption of coyotes in the social condition can be given as follows:

$$zks_b^{o,s} = z(sco_b^{o^{th},s^{th}}) \quad (6)$$

Initially, the coyotes are allotted to a group. Moreover, they can be removed and combined into packages or remain individual. The probability of a coyote being rejected from the group is  $O_B$  as shown in Eq. (7).

$$O_E = 1.005 \cdot R_b^2 \quad (7)$$

This method is used with the COA algorithm to interconnect with the entire population of coyotes. This group contains two alphas, while the COA takes only one alpha. In the event of minimization, the alpha of  $o^{th}$  pack in the instant time  $s^{th}$  is shown in Eq. (8).

$$alpha^{o,s} = \{sco_b^{o,s} | arg_{b=\{1,2,\dots,R_b\}} \min z(sco_b^{o,s})\} \quad (8)$$

$$cult_n^{o,s} = \begin{cases} T_{\frac{o,s(R_b+1)}{2}, n'}, & R_b \text{ odd} \\ T_{\frac{R_b o,s}{2}, n'} + T_{\frac{o,s(R_b+1)}{2}, n'}, & \text{otherwise} \end{cases} \quad (9)$$

The parameter  $T^{o,s}$  denotes the social circumstance of coyotes to  $0^{th}$  a group at the instant time  $s^{th}$  for every  $n$  within  $[0, F]$ .

The age of coyote can be denoted as  $age_b^{o,s} \in R$ , the birth of a new coyote can be indicated as the consolidation of two parents' social circumstances in the inspired environment, as follows.

$$pup_n^{o,s} = \begin{cases} soc_{u1,n}^{o,s}, & urf_n < O_c \text{orn} = n_1 \\ soc_{u2,n}^{o,s}, & urf_n > O_c + O_x \text{orn} = n_2 \\ U_n, & \text{otherwise} \end{cases} \quad (10)$$

The variables  $u_1$  and  $u_2$  are denoted as the arbitral coyotes from the  $0^{th}$  group, the arbitral dimensions are correspondingly represented as  $n_1$  and  $n_2$  then  $O_c$  is represented as the uniform probability distribution,  $U_n$  shows the random integer in the decision term bounds of  $n^{th}$  dimension and  $urf_n$  Indicates the random value within  $[0,1]$ , generated by the uniform probability. The culture diversity of coyotes is trained with scatter and association probability.

$$O_c = \frac{1}{F} \quad (11)$$

$$O_x = \frac{1-O_c}{2} \quad (12)$$

The parameter  $O_c$  is used to characterize scatter probability distribution,  $O_x$  denotes the uniform probability. The term  $F$  denotes the search gap dimension.

Now,  $\omega$  and  $\gamma$  variables represent corresponding packs of coyotes in weak conditions. The COA signifies coyotes in pack influence ( $\delta_b$ ) and alpha influence ( $\delta_a$ ). The parameter  $bu_1$  represent the random coyote of the groups to the alpha coyote, and  $bu_2$  the random coyote culture compared to the actual behaviours of the group. The random coyote was correspondingly selected from a uniform probability  $\delta_a$  and  $\delta_b$ , as follows.

$$\delta_1 = cult^{o,s} - sco_{bu_1}^{o,s} \quad (13)$$

$$\delta_2 = cult^{o,s} - sco_{bu_2}^{o,s} \quad (14)$$

Thus, the alpha and park influences update the novel social circumstance of coyote as follows.

$$new\_sco_b^{o,s} = sco_b^{o,s} + u_1\delta_a + u_2\delta_2 \quad (15)$$

The parameters  $u_1$  and  $u_2$  are the uniformly distributed random number between zero and one. The new social circumstance is shown in Eq. (16).

$$new\_fit_b^{o,s} = z(new\_sco_b^{o,s}) \quad (16)$$

Lastly, the social circumstance of coyote's is given in Eq. (17) and applied to global optimization issues.

$$sco_b^{o,s+1} = \begin{cases} new\_sco_b^{o,s}, & new\_fit_b^{o,s} < fit_b^{o,s} \\ sco_b^{o,s}, & otherwise \end{cases} \quad (17)$$

The COA derives a fitness function with the maximization of PSNR. It can be represented as follows.

$$fitness = \max \{PSNR\} \quad (18)$$

### 3.4. Embedding and Extraction Process

The frames can be separated as  $U, V, Y$  channels, and because of their optimum perceptibility, the  $U$  channel can be chosen as an embedded place. The 3-stage DTCWT changed to (a) decompose  $U$  as one low-pass sub band and six high-pass sub bands. All the sub-bands can be compared in several directions. Consider that video with  $k$  framing, the high-pass subband from the  $k^{th}$  frame, then DTCWT decomposition is defined as  $U_{l,d}^{H,k}$ . The low-pass subband can be defined as  $U^L$ , and SVD-EVD conversion has been carried out on all the high-pass subbands correspondingly. The singular value of the high-pass sub band as candidate co-efficient can be defined as  $SV_d^{i,d}$ . The candidate co-efficient can be measured as:

$$U_d^{i,k} (SV_d^{i,k}) V_d^{i,kT} = SVD(U_{3,d}^{H,k}) \quad (19)$$

## 4. Results and Discussion

This study investigates the achievement of the COA-hybrid model on five benchmark images. Fig. 3 demonstrates the sample images.

Fig. 4 visualizes the generated watermarked images generated by the COA-hybrid approach on 25 iterations. The watermarked images showed that the COA-hybrid method has effectually embedded the watermarks on different iterations. Fig. 5 visualizes the extracted watermarked images acquired by the COA-hybrid method on 25 iterations. The extracted images display that the COA-hybrid method has effectually extracted the watermark image on different iterations.

Table 1 and Fig. 6 demonstrate the overall watermarking results of the COA-hybrid model under different iterations. The results indicate that the COA-hybrid model increases PSNR, SSIM, and NCC values [27]. At the same time, the COA-hybrid model obtains decreasing RMSE and MSE values.

Table 2 demonstrates the entire outcomes of the COA-hybrid approach under five images. In Fig. 7, the outcomes of the COA-hybrid model are examined by means of MSE and RMSE. The results identified that the COA-hybrid model attained effectual outcomes on all images regarding MSE and RMSE.

Based on MSE, the COA-hybrid model offers MSE of 0.008, 0.011, 0.002, 0.015, and 0.037 under images 1-5, respectively. Besides, depending on RMSE, the COA-hybrid technique offers RMSE of 0.089, 0.106, 0.040, 0.121, and 0.192 under images 1-5.

In Fig. 8, the results of the COA-hybrid method are examined using PSNR. The outcomes recognized that the

COA-hybrid approach obtained effectual outcomes on all images in terms of PSNR. Based on PSNR, the COA-hybrid method offers PSNR of 69.144dB, 67.655dB, 76.210dB, 66.491dB, and 62.476dB under images 1-5 correspondingly.

In Fig. 9, the outputs of the COA-hybrid model are examined by means of SSIM. The results recognized that the COA-hybrid method attained effectual outcomes on all images regarding SSIM. Based on SSIM, the COA-hybrid model offers SSIM of 100%, 100%, 100%, 100%, and 100% under images 1-5 correspondingly.

Table 3 and Fig. 10 show a detailed PSNR study of the COA-hybrid model with recent models [25]. The experimental values indicate that the PSO-DIW technique reaches the least PSNR values. The CSO-DIW, FA-DIW, and MOACO-DIW techniques also obtain moderately closer PSNR values. However, the COA-hybrid model attains superior performance with increased PSNR values of 69.144dB, 56.732dB, 53.821dB, 50.757dB, 52.849dB, and 44.662 dB. These results confirmed the enhanced outcomes of the COA-hybrid model compared to other models.

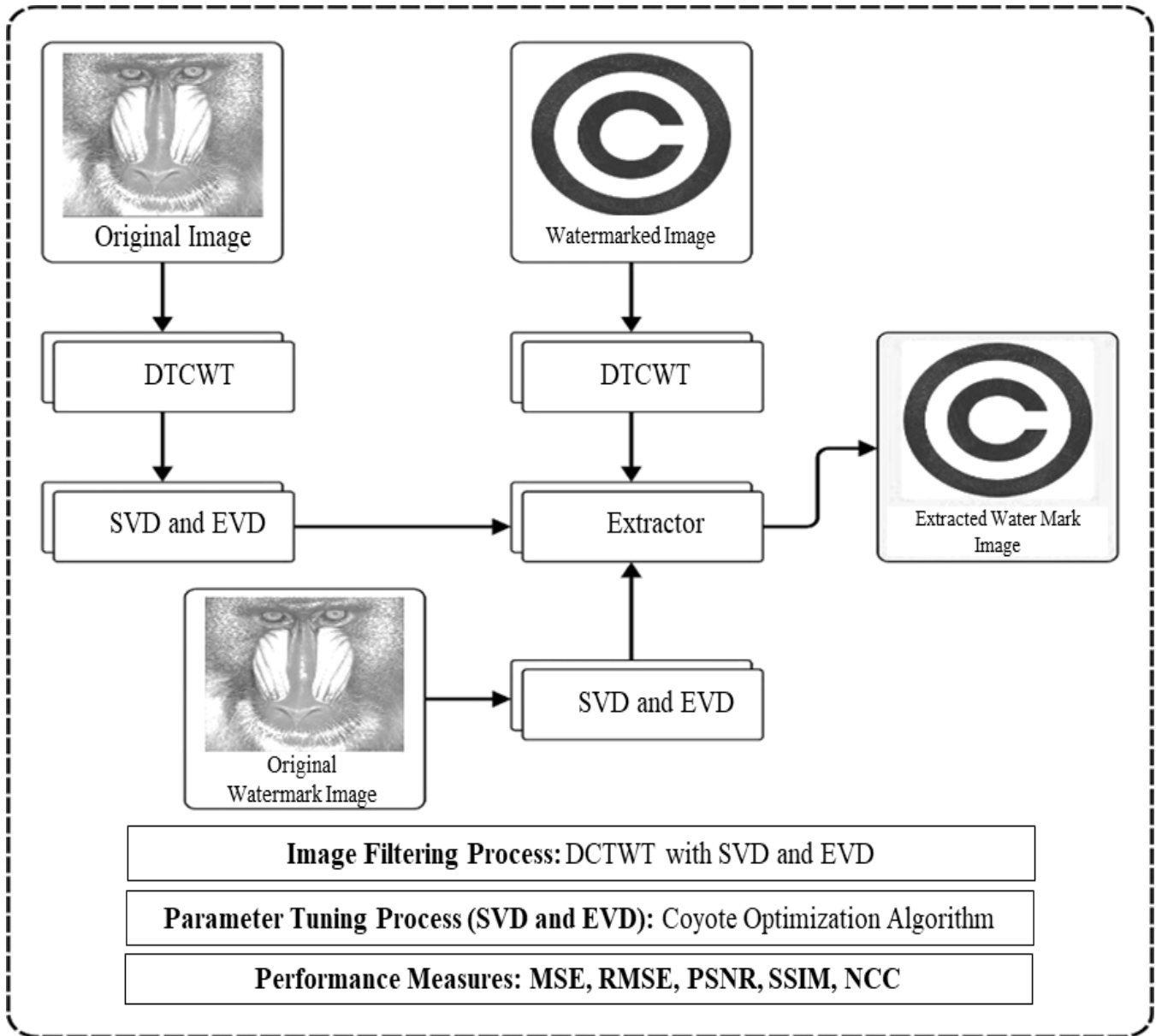


Fig. 1 Overall process of COA-hybrid approach

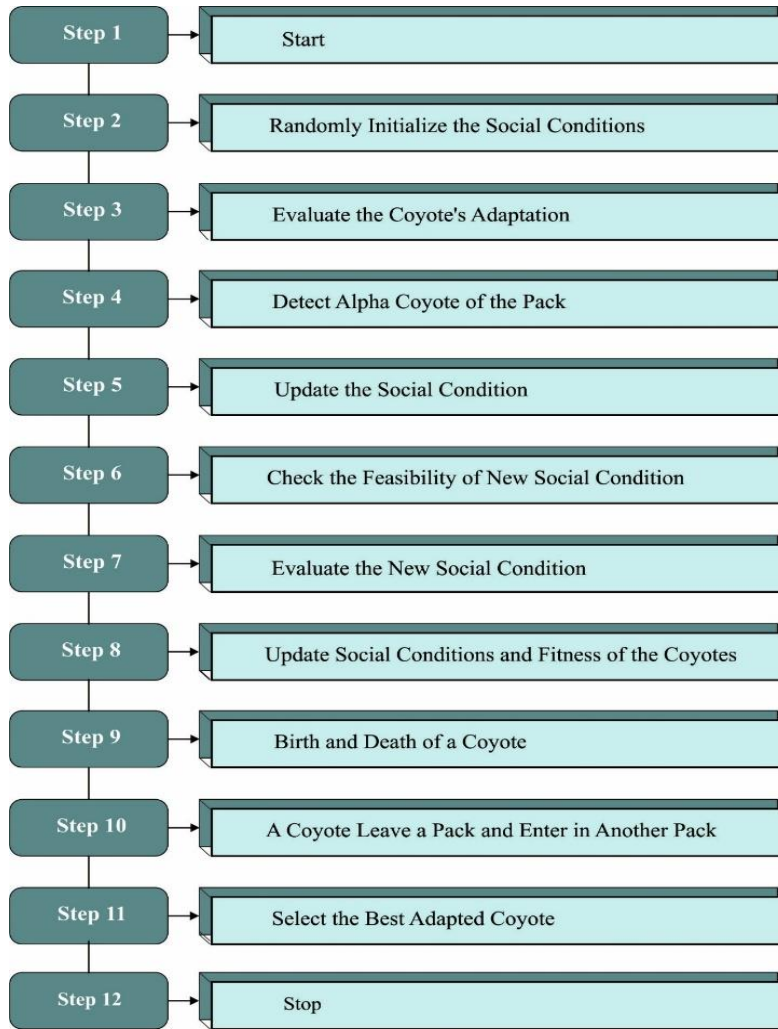


Fig. 2 Steps included in COA

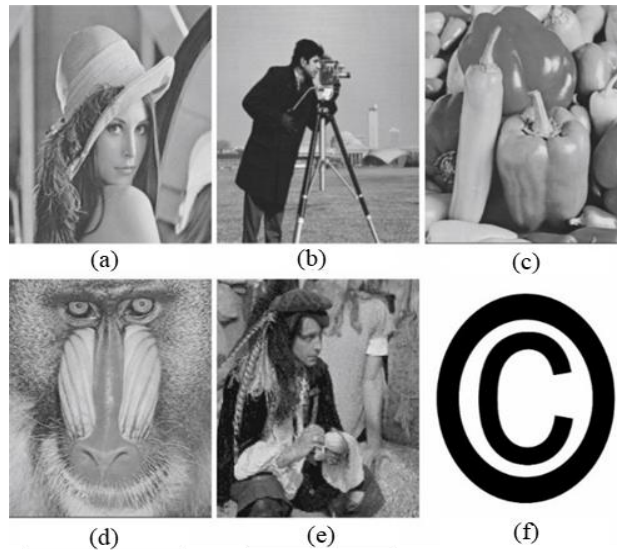


Fig. 3 Sample imageries (a) Lena (b) Cameraman (c) Peppers (d) Baboon (e) Man (f) Secret image

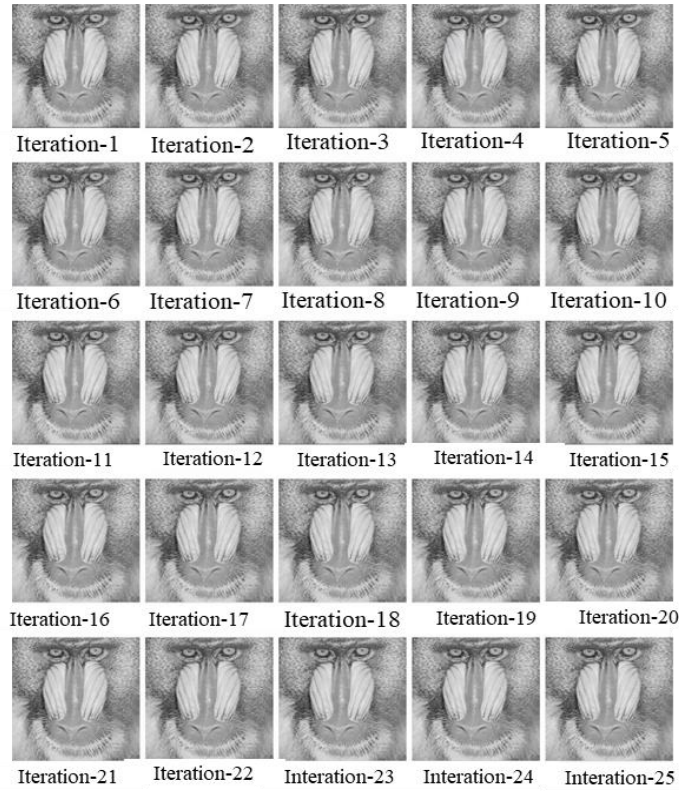


Fig. 4 Watermarked images on 25 iterations

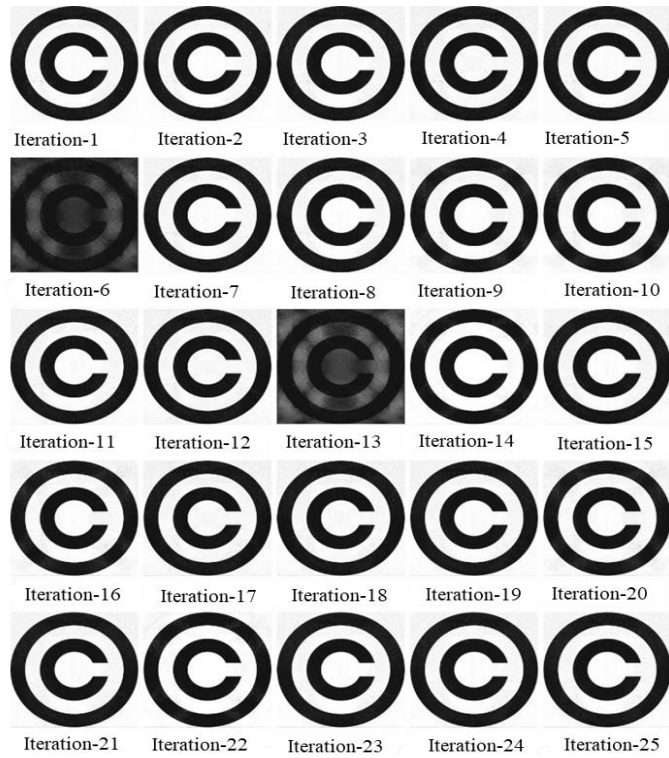
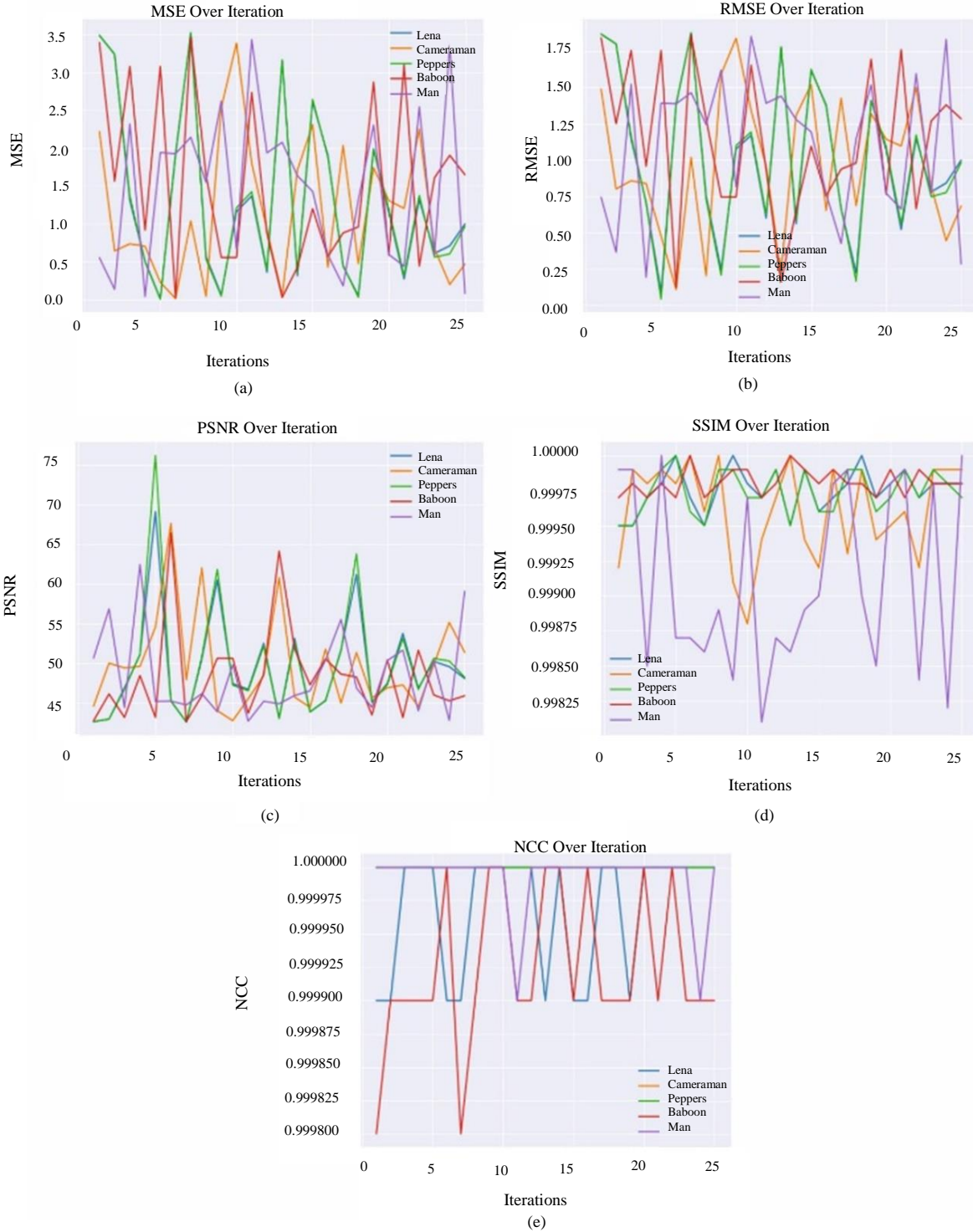


Fig. 5 Extracted watermarked images on 25 iterations

**Table 1. Watermarking outcomes of the COA-hybrid approach under varying iterations**

<b>Iterations</b>	<b>MSE</b>	<b>RMSE</b>	<b>PSNR</b>	<b>SSIM</b>	<b>NCC</b>
1	3.3939	1.8423	42.8238	0.9997	0.9998
2	1.5631	1.2502	46.1910	0.9998	0.9999
3	3.0796	1.7549	43.2458	0.9997	0.9999
4	0.9155	0.9568	48.5140	0.9998	0.9999
5	3.0804	1.7551	43.2448	0.9997	0.9999
6	0.0146	0.1208	66.4910	1.0000	1.0000
7	3.4641	1.8612	42.7348	0.9997	0.9998
8	1.6462	1.2831	45.9659	0.9998	0.9999
9	0.5549	0.7449	50.6886	0.9999	1.0000
10	0.5545	0.7446	50.6918	0.9999	1.0000
11	2.7351	1.6538	43.7611	0.9997	0.9999
12	0.8741	0.9349	48.7151	0.9998	0.9999
13	0.0249	0.1578	64.1711	1.0000	1.0000
14	0.4238	0.6510	51.8591	0.9999	1.0000
15	1.1980	1.0945	47.3463	0.9998	0.9999
16	0.5656	0.7520	50.6059	0.9999	1.0000
17	0.8777	0.9369	48.6974	0.9998	0.9999
18	0.9584	0.9790	48.3154	0.9998	0.9999
19	2.8712	1.6944	43.5502	0.9997	0.9999
20	0.5809	0.7622	50.4899	0.9999	1.0000
21	3.0978	1.7600	43.2203	0.9997	0.9999
22	0.4398	0.6632	51.6986	0.9999	1.0000
23	1.6080	1.2681	46.0680	0.9998	0.9999
24	1.9038	1.3798	45.3346	0.9998	0.9999
25	1.6477	1.2836	45.9620	0.9998	0.9999



**Fig. 6** Watermarking outcome of COA-hybrid method (a) MSE, (b) RMSE, (c) PSNR, (d) SSIM, and (e) NCC

**Table 2. Classifier outcome of COA-hybrid method under five images**

Number of Images	MSE	RMSE	PSNR	SSIM	NCC
Image-1 (Lena)	0.008	0.089	69.144	100	1.000
Image-2 (Cameraman)	0.011	0.106	67.655	100	1.000
Image-3 (Peppers)	0.002	0.040	76.210	100	1.000
Image-4 (Baboon)	0.015	0.121	66.491	100	1.000
Image-5 (Man)	0.037	0.192	62.476	100	1.000

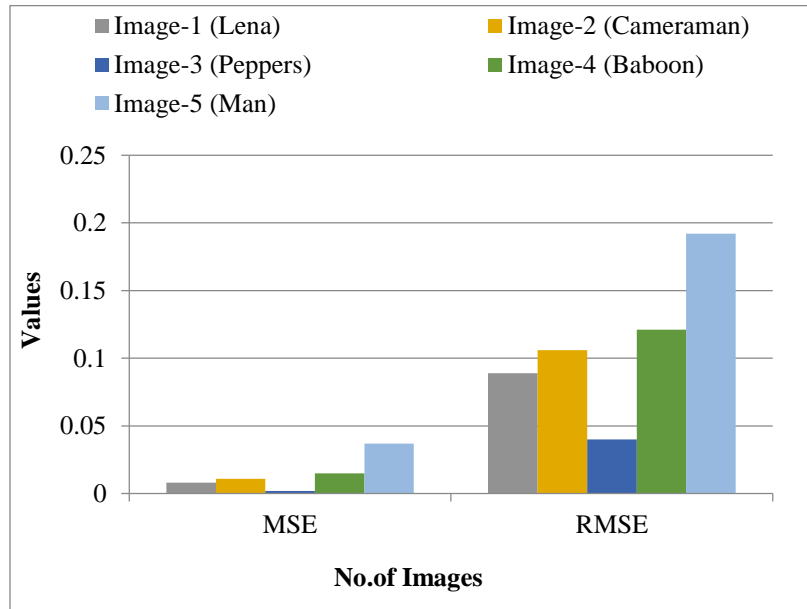


**Fig. 7 MSE and RMSE analysis of COA-hybrid technique under distinct images**

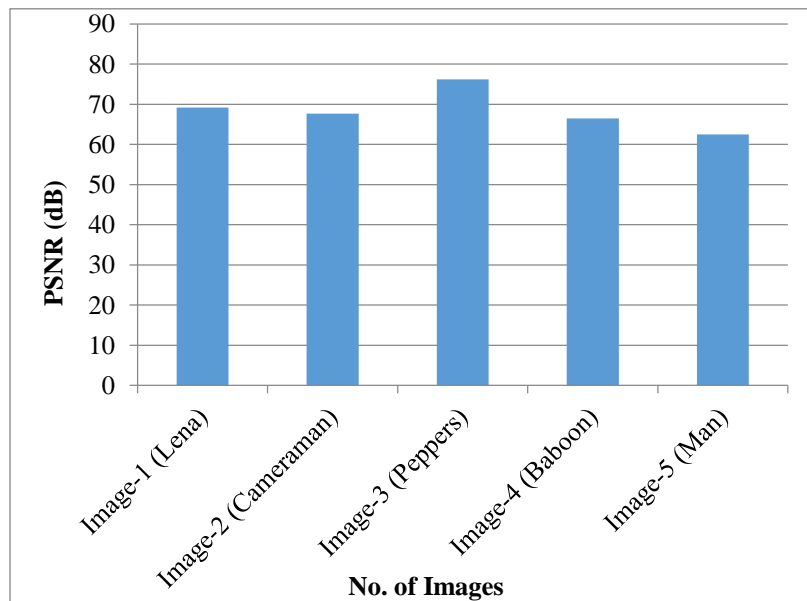


**Fig. 8 PSNR analysis of COA-hybrid technique under distinct images**

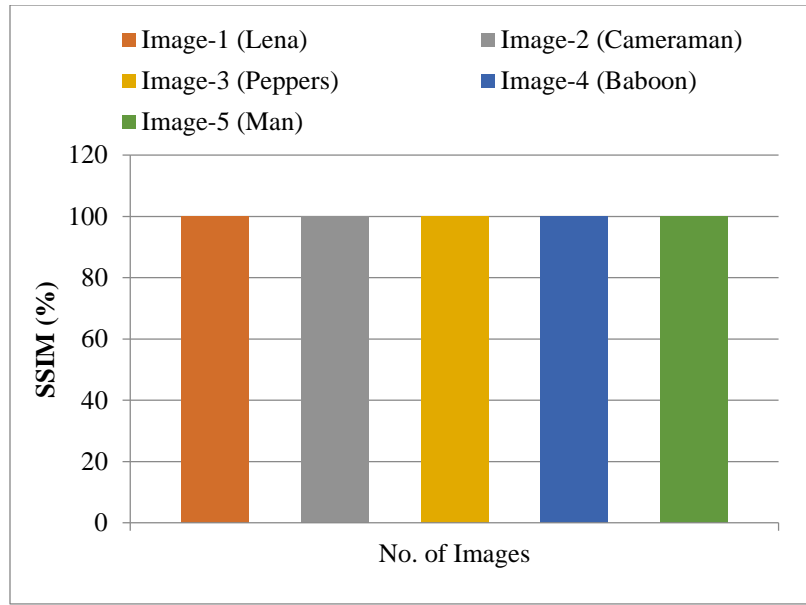


Fig. 9 SSIM analysis of COA-hybrid technique under distinct images

Table 3. PSNR analysis of COA-hybrid approach with other recent algorithms

PSNR (dB)					
Methods	1 <sup>st</sup> Image	2 <sup>nd</sup> Image	3 <sup>rd</sup> Image	4 <sup>th</sup> Image	5 <sup>th</sup> Image
COA-Hybrid Model	69.144	67.655	76.210	66.491	62.476
SWT-MGWO	56.732	58.354	57.127	56.577	56.428
CSO-DIW	53.821	53.231	55.201	52.926	52.440
FA-DIW	50.757	51.574	53.555	55.370	51.093
MOACO-DIW	52.849	54.480	48.992	48.178	50.741
PSO-DIW	44.662	50.349	49.290	48.665	51.030



Fig. 10 PSNR analysis of COA-hybrid approach with other recent algorithms

## 5. Conclusion

In this study, we have developed a novel COA-hybrid model for the digital Image watermarking procedure. The presented COA-hybrid technique lies in developing an effective Image watermarking approach to fulfil the requirements of imperceptibility and robustness. Besides, the COA-hybrid model integrates the concepts of the SVD and EVD approaches. Moreover, the COA-hybrid technique

embeds the watermarking technique on the DWT subband of the cover image. Furthermore, the watermarks are placed on the particular value components of the DWT subband of the cover image. Finally, the COA is utilized to adjust the parameters related to the hybrid model to increase fitness function. The simulation results of the COA-hybrid model are tested on different images, and the results reported the improvements of the COA-hybrid model over other models.

## References

- [1] ErtugrulGul, and AhmetNusretToprak, "Contourlet and Discrete Cosine Transform-Based Quality Guaranteed Robust Image Watermarking Method using Artificial Bee Colony Algorithm," *Expert Systems with Applications*, vol. 212, p. 118730, 2023. [[CrossRef](#)] [[Google Scholar](#)] [[Publisher Link](#)]
- [2] NkwachukwuChukwuchekwa, BukolaAkinwola, and James Onojo, "Improved DCT Based Digital Image Watermarking Technique using Particle Swarm Optimization Algorithm," *International Research Journal of Engineering and Technology (IRJET)*, vol. 6, no. 1, pp. 2395-0056, 2019. [[Google Scholar](#)] [[Publisher Link](#)]
- [3] Lei Wang, and HuichaoJi, "A Watermarking Optimization Method based on Matrix Decomposition and DWT for Multi-Size Images," *Electronics*, vol. 11, no. 13, p. 2027, 2022. [[CrossRef](#)] [[Google Scholar](#)] [[Publisher Link](#)]
- [4] Zaid Bin Faheem et al., "Image Watermarking using Least Significant Bit and Canny Edge Detection," *Sensors*, vol. 23, no. 3, p. 1210, 2023. [[CrossRef](#)] [[Google Scholar](#)] [[Publisher Link](#)]
- [5] Jae-Eun Lee et al., "Digital Image Watermarking Processor Based on Deep Learning," *Electronics*, vol. 10, no. 10, p. 1183, 2021. [[CrossRef](#)] [[Google Scholar](#)] [[Publisher Link](#)]
- [6] Parmalik Kumar, and A. K. Sharma, "A Robust Image Watermarking Technique using Feature Optimization and Cascaded Neural Network," *International Journal of Computer Science and Information Security (IJCSIS)*, vol. 18, no. 8, pp. 36-45, 2019. [[Google Scholar](#)] [[Publisher Link](#)]
- [7] Vipul Sharma, and Roohie Naaz Mir, "An Enhanced Time Efficient Technique for Image Watermarking using Ant Colony Optimization and Light Gradient Boosting Algorithm," *Journal of King Saud University-Computer and Information Sciences*, vol. 34, no. 3, pp. 615-626, 2022. [[CrossRef](#)] [[Google Scholar](#)] [[Publisher Link](#)]
- [8] TaybehSalehnia, and AbdolhosseinFathi, "Fault Tolerance in LWT-SVD Based Image Watermarking Systems using Three Module Redundancy Technique," *Expert Systems with Applications*, vol. 179, p. 115058, 2021. [[CrossRef](#)] [[Google Scholar](#)] [[Publisher Link](#)]
- [9] Osama R. Shahin, Zeinab M. Abdel Azim, and Ahmed I Taloba, "Maneuvering Digital Watermarking in Face Recognition," *International Journal of Engineering Trends and Technology*, vol. 69, no. 11, pp. 104-112, 2021. [[CrossRef](#)] [[Google Scholar](#)] [[Publisher Link](#)]
- [10] Tushar Debnath, Surajit Paul, and Kumar Amitabh, "Image Restoration Quality Measurement using Noise Filters," *SSRG International Journal of Electronics and Communication Engineering*, vol. 10, no. 2, pp. 1-5, 2023. [[CrossRef](#)] [[Publisher Link](#)]
- [11] Venkat P. Patil, and C. Ram Singla, "Performance Enhancement of Image Stitching Process under Bound Energy Aided Feature Matching and Varying Illumination Environments," *SSRG International Journal of Electronics and Communication Engineering*, vol. 6, no. 9, pp. 1-6, 2019. [[CrossRef](#)] [[Google Scholar](#)] [[Publisher Link](#)]
- [12] KarimanMamdouh, Noura A. Semary, and Hatem Ahmed, "A Blind Fragile Watermarking for a 3D Triangular Model Based on Curvature Features and Chaos Sequence," *IJCI International Journal of Computers and Information*, vol. 9, no. 2, pp. 14-24, 2022. [[CrossRef](#)] [[Google Scholar](#)] [[Publisher Link](#)]
- [13] Mourad R. Mouhamed et al., "Watermarking 3D Printing Data Based on Coyote Optimization Algorithm," *Machine Learning and Big Data Analytics Paradigms: Analysis, Applications and Challenges*, vol. 77, pp. 603-624, 2020. [[CrossRef](#)] [[Google Scholar](#)] [[Publisher Link](#)]
- [14] Rayappa David Amar Raj, and Kanasottu Anil Naik, "Optimal Reconfiguration of PV Array Based on Digital Image Encryption Algorithm: A Comprehensive Simulation and Experimental Investigation," *Energy Conversion and Management*, vol. 261, p. 115666, 2022. [[CrossRef](#)] [[Google Scholar](#)] [[Publisher Link](#)]
- [15] M. Sajeer, and Ashutosh Mishra, "A Robust and Secured Fusion Based Hybrid Medical Image Watermarking Approach using RDWT-DWT-MSVD with Hyperchaotic System-Fibonacci Q Matrix Encryption," *Multimedia Tools and Applications*, pp. 1-23, 2023. [[CrossRef](#)] [[Google Scholar](#)] [[Publisher Link](#)]
- [16] Junxiu Liu et al., "An Optimized Image Watermarking Method Based on HD and SVD in DWT Domain," *IEEE Access*, vol. 7, pp. 80849-80860, 2019. [[CrossRef](#)] [[Google Scholar](#)] [[Publisher Link](#)]

- [17] Manuel Cedillo-Hernandez, Antonio Cedillo-Hernandez, and Francisco J. Garcia-Ugalde, "Improving DFT-Based Image watermarking using Particle Swarm Optimization Algorithm," *Mathematics*, vol. 9, no. 15, p. 1795, 2021. [[CrossRef](#)] [[Google Scholar](#)] [[Publisher Link](#)]
- [18] KilariJyothsna Devi et al., "A New Robust and Secure 3-Level Digital Image Watermarking Method Based on G-BAT Hybrid Optimization," *Mathematics*, vol. 10, no. 16, p. 3015, 2022. [[CrossRef](#)] [[Google Scholar](#)] [[Publisher Link](#)]
- [19] K. Jyothsna Devi et al., "Robust and Secured Watermarking using Ja-Fi Optimization For Digital Image Transmission in Social Media," *Applied Soft Computing*, vol. 131, p. 109781, 2022. [[CrossRef](#)] [[Google Scholar](#)] [[Publisher Link](#)]
- [20] Vijay Krishna Pallaw et al., "A Robust Medical Image Watermarking Scheme Based on Nature-Inspired Optimization for Telemedicine Applications," *Electronics*, vol. 12, no. 2, p. 334, 2023. [[CrossRef](#)] [[Google Scholar](#)] [[Publisher Link](#)]
- [21] El-Sayed M. El-Kenawy et al., "Advanced Dipper-Throated Meta-Heuristic Optimization Algorithm for Digital Image Watermarking," *Applied Sciences*, vol. 12, no. 20, p. 10642, 2022. [[CrossRef](#)] [[Google Scholar](#)] [[Publisher Link](#)]
- [22] Yifei Wang et al., "A DTCWT-SVD Based Video Watermarking Resistant to Frame Rate Conversion," *In 2022 International Conference on Culture-Oriented Science and Technology (CoST)*, pp. 36-40, 2022. [[CrossRef](#)] [[Google Scholar](#)] [[Publisher Link](#)]
- [23] Dinesh P S et al., "Digital Fragile Watermarking Video Based on Discrete Wavelet Transformation," *SSRG International Journal of Computer Science and Engineering*, vol. 6, no. 11, pp. 5-9, 2019. [[CrossRef](#)] [[Publisher Link](#)]
- [24] Mokhtar Hussein, and B. Manjula, "A Hybrid Approach for SVD and Neural Networks Based Robust Image Watermarking," *International Journal of P2P Network Trends and Technology*, vol. 61, no. 2, pp. 117-121, 2018. [[CrossRef](#)] [[Publisher Link](#)]
- [25] R. Iniyavan, and B. Vijayalakshmi, "Design and Development of Improved Coyote Optimization-Based Adaptive Equalization Technique for ECG Signal Transmission," *ECTI Transactions on Electrical Engineering, Electronics, and Communications*, vol. 21, no. 1, pp. 248608-248608, 2023. [[CrossRef](#)] [[Google Scholar](#)] [[Publisher Link](#)]
- [26] Snehlata Maloo, Mahendra Kumar, and N. Lakshmi, "A Modified Whale Optimization Algorithm Based Digital Image Watermarking Approach," *Sensing and Imaging*, vol. 21, no. 26, pp. 1-22, 2020. [[CrossRef](#)] [[Google Scholar](#)] [[Publisher Link](#)]
- [27] SonileKatungulaMusonda, and John Soraghan, "Digital Image Watermarking in the Discrete Wavelet Domain and Analysis of the Effects of Compression on Watermarked Images," *SSRG International Journal of Electrical and Electronics Engineering*, vol. 2, no. 12, pp. 1-14, 2015. [[CrossRef](#)] [[Publisher Link](#)]
- [28] S.Jagadeesan, and P.Jaisankar, "Fused Distortion Measurement For Securing Rgb Steganography," *International Journal of Engineering Trends and Technology*, vol. 68, no. 3, pp. 64-68, 2020. [[CrossRef](#)] [[Google Scholar](#)] [[Publisher Link](#)]